

# Programmable Superpositions of Ising Configurations

Lukas M. Sieberer<sup>1</sup> and Wolfgang Lechner<sup>2,3,\*</sup>

<sup>1</sup>*Department of Physics, University of California, Berkeley, California 94720, USA*

<sup>2</sup>*Institute for Theoretical Physics, University of Innsbruck, A-6020 Innsbruck, Austria*

<sup>3</sup>*Institute for Quantum Optics and Quantum Information of the Austrian Academy of Sciences, A-6020 Innsbruck, Austria*

(Dated: July 8, 2022)

We present a framework to prepare superpositions of bit strings, i.e., many-body spin configurations, with deterministic programmable probabilities. The spin configurations are encoded in the degenerate ground states of the lattice-gauge representation of an all-to-all connected Ising spin glass. The ground state manifold is invariant under variations of the gauge degrees of freedom, which take the form of four-body parity constraints. Our framework makes use of these degrees of freedom by individually tuning them to dynamically prepare programmable superpositions. The dynamics combines an adiabatic protocol with controlled diabatic transitions. We derive an effective model that allows one to determine the control parameters efficiently even for large system sizes.

PACS numbers: 03.67.Ac,03.65.Ud,03.67.Bg

*Introduction.*—The realization of quantum many-body superpositions is a cornerstone of current developments in quantum simulation experiments [1–8]. The aim is to achieve deterministic tunability over individual constituents of the quantum state in an experiment. Superpositions of bit strings (encoded in spin configurations) have been recently proposed as a key to quantum machine learning applications [9–11]. From an experimental point of view, the technique of adiabatic state preparation of spin models [12–15], which recently gained considerable interest as a tool to solve optimization problems, might serve as an effective method to prepare such states. If the ground state of the final Hamiltonian in an adiabatic protocol is energetically degenerate, the final state of the protocol is a superposition of the configurations in the degenerate manifold [16, 17]. However, the amplitudes of this state are governed by the details of the dynamics and the population can be exponentially biased [18], leaving open the challenge to deterministically program these probabilities.

In this Letter, we introduce a framework to generate superpositions of arbitrary bit strings with programmable squared amplitudes via an adiabatic-diabatic state preparation. The  $M$  different bit strings of length  $N$  are encoded in the ground state of the lattice-gauge representation of an all-to-all connected Ising model with  $K$  spins [19]. We show that the gauge degrees of freedom in this representation, i.e., the constraints, allow one to shape the quantum dynamics and program the final amplitudes. We develop an effective  $M$ -dimensional theory. In the reduced Hilbert space of the effective model, the parameters can be determined efficiently, even for system sizes that cannot be solved on current classical computers (i.e., more than 50 qubits).

The basis of the protocol is the lattice-gauge represen-

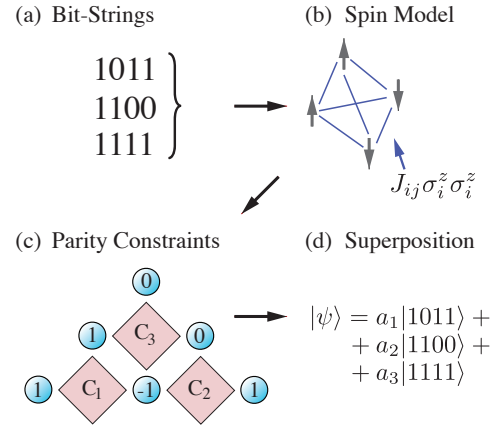


Figure 1. Schematic outline of the protocol to store classical bit strings in a quantum superposition with programmable probabilities  $|a_n|^2$ . (a) The input are  $M$  classical bit strings. (b) An all-to-all connected classical spin model with Hamiltonian  $H = \sum_{i,j} J_{ij} \sigma_i^z \sigma_j^z$  is constructed such that the bit strings are its degenerate ground states. (c) The spin model is translated to a lattice gauge model with qubits (blue spheres) and with four-body constraint strengths  $C_p$  (red squares) [19]. (d) The adiabatic passage of this model yields a superposition of the  $M$  degenerate ground states. The probabilities that can be tuned on demand by choosing the values of the  $C_p$  appropriately.

tation of an all-to-all connected spin model [19–23]

$$H(t) = -A(t) \sum_{i=1}^K \sigma_i^x - B(t) \sum_{i=1}^K J_i \sigma_i^z - C(t) \sum_{p=1}^{K-N+1} C_p \sigma_{n_p}^z \sigma_{w_p}^z \sigma_{s_p}^z \sigma_{e_p}^z. \quad (1)$$

Here,  $\sigma_i^{x,y,z}$  are the Pauli operators,  $K = N(N-1)/2$ , and the sum in the last term runs over the  $K-N+1$  constraints. Each constraint with index  $p$  involves the spins

in the north, west, south, and east of the constraint site, as is indicated in Eq. (1) with subscripts  $n_p, w_p, s_p$ , and  $e_p$ . The functions  $A(t) = t/T$  and  $B(t) = C(t) = 1 - t/T$  are linear switching functions, and  $T$  is the run time of the protocol. Initially,  $A(0) = 1$  and  $B(0) = C(0) = 0$  while at the end of the protocol  $A(T) = 0$  and  $B(T) = C(T) = 1$ . We measure energies (and inverse times) in units of the transverse field strength, which is thus set to one. The qubits in Eq. (1) represent connections between logical spins of the all-to-all connected Ising model. The mapping to the lattice-gauge representation introduces additional degrees of freedom, which are removed by the constraints in the last term of Eq. (1) (see Ref. [19] for details). The constraint strengths  $C_p$  are gauge degrees of freedom. Tuning each of them individually does not change the low-energy subspace in the final Hamiltonian in which the bit strings are encoded. Thus, the model features  $(N - 2)(N - 3)/2$  additional parameters. We use these additional parameters to systematically design the quantum paths of an adiabatic-diabatic protocol, which allows one to program the squared amplitudes of the configurations in the final state.

Our protocol, illustrated in Fig. 1, aims at storing arbitrary bit strings  $\{x_1, x_2, \dots\}$  as a superposition  $|\psi\rangle = a_1|x_1\rangle + a_2|x_2\rangle + \dots$  with programmable probabilities  $p_n = |a_n|^2$ . We regard the states  $|x_n\rangle = |01011\dots\rangle$  as product states in the  $\sigma^z$  basis, with individual bits  $x_{n,i} = 0, 1$  corresponding to eigenvalues  $\pm 1$  of  $\sigma_i^z$ . The protocol consists of the following steps: (i) The bit strings are encoded as degenerate ground states of a classical spin model [see Fig. 1 (a) and (b)]. This is achieved with a Hamiltonian of the form  $H = \sum_{n=1}^M |x_n\rangle\langle x_n|$  which can be approximated, for example, via plated solutions [24] or Hopfield networks [25] in the form of an all-to-all connected model with energy  $\sum_{i,j} J_{ij}\sigma_i^z\sigma_j^z$ . The details of different strategies of this classical encoding will be discussed elsewhere [26]. (ii) This spin Hamiltonian is reformulated in the parity-constraint model introduced in Ref. [19] with Hamiltonian  $H(t)$  in Eq. (1) [see Fig. 1 (c)]. Logical bit strings  $x_n$  are thus translated to physical bit strings  $z_n$ , representing spin configurations in the lattice-gauge model. (iii) The key step, and focus of this work, is the dynamics that leads to the desired superposition. The system is initialized in the trivial and non-degenerate ground state of  $H(0)$ , in which all spins are aligned by the transverse field. Evolution with  $H(t)$  yields a superposition of all configurations in the ground state manifold of  $H(T)$ ,  $|\psi\rangle = \sum_{n=1}^M a_n |z_n\rangle$ , where the probabilities  $|a_n|^2$  can be tuned on demand by adjusting the parameters  $C_p$ . These parameters  $C_p$  are determined from static properties of an effective Hamiltonian, and can be fine-tuned via an iterative protocol.

*Effective model.*—The quantum adiabatic algorithm with a single non-degenerate ground state of the “problem Hamiltonian”  $H(T)$  is successful if adiabaticity is

maintained throughout the time evolution. Here, in contrast, we consider the case of an  $M$ -fold degenerate ground state manifold of the problem Hamiltonian [18]. Thus, the gap closes as  $t \rightarrow T$  and the dynamics can never be fully adiabatic. Nevertheless, by making  $T$  large, transitions out of the *adiabatic manifold* (AMF), which is spanned by the  $M$  lowest-lying instantaneous eigenstates  $\{|\varphi_n(t)\rangle \mid n = 1, \dots, M\}$  of  $H(t)$  and evolves for  $t \rightarrow T$  into the degenerate ground state manifold of  $H(T)$ , are suppressed. Our protocol aims at controlling the *diabatic dynamics within the AMF* by tuning the constraint strengths  $C_p$ . In this sense, the final state is prepared *adiabatic-diabatically*.

Within the AMF, the dynamics consists of two different regimes: up to a characteristic time  $t_d$  the dynamics is adiabatic and the system remains in the instantaneous ground state  $|\varphi_1(t)\rangle$ ; from  $t_d$  to  $T$  the dynamics can be considered as a sudden quench of the Hamiltonian parameters, during which the state of the system  $|\psi(t)\rangle$  essentially remains frozen, i.e.,  $|\psi(T)\rangle \approx |\psi(t_d)\rangle \approx |\varphi_1(t_d)\rangle$ . (In the last equality, we omitted dynamical and Berry phases since we are interested solely in programming the *probabilities* of the final superposition state.) A detailed discussion of this Kibble-Zurek-inspired [27] approximation in the context of the Landau-Zener problem is provided in Ref. [28]. The *dynamical* problem of controlling diabatic transitions is thus approximately reduced to the *static* problem of choosing the constraint strengths  $C_p$  to tune the composition of the instantaneous ground state at time  $t_d$ . Below, we derive the effective Hamiltonian  $H_{\text{eff}}(t)$  in the AMF that allows us to do this efficiently.

A state in the AMF can be written as  $|\psi(t)\rangle = \sum_{n=1}^M \alpha_n(t) |\varphi_n(t)\rangle$ , and the Schrödinger equation, projected on the AMF, takes the form

$$i\dot{\alpha}_n = \sum_{n'=1}^M A_{nn'} \alpha_{n'}, \quad A_{nn'} = \langle \varphi_n | \left( H - i \frac{d}{dt} \right) | \varphi_{n'} \rangle. \quad (2)$$

In order to find the instantaneous eigenstates that determine  $A_{nn'}$ , we first apply a Schrieffer-Wolff (SW) transformation  $U_{\text{SW}}(t)$  [29] to decouple the AMF from higher-lying excited states, and then we diagonalize the resulting effective Hamiltonian  $H_{\text{eff}}(t) = U_{\text{SW}}(t)H(t)U_{\text{SW}}^\dagger(t)$  within the AMF by another unitary transformation  $U_0(t)$ . As a result,  $|\varphi_n(t)\rangle = U_{\text{SW}}^\dagger(t)U_0^\dagger(t)|z_n\rangle$ , and inserting this representation in Eq. (2) we obtain

$$A_{nn'} = \langle z_n | \left[ U_0 \left( H_{\text{eff}} - iU_{\text{SW}}\dot{U}_{\text{SW}}^\dagger \right) U_0^\dagger - iU_0\dot{U}_0^\dagger \right] | z_{n'} \rangle. \quad (3)$$

The SW transformation can be constructed systematically by treating the transverse field as a perturbation [29]. This is justified since diabatic transitions occur only in later stages of the time evolution when the amplitude of the transverse field  $A(t) = 1 - t/T$  in Eq. (1) is small. We emphasize that we use perturbation theory

only to solve the *static* problem of finding the instantaneous eigenstates of  $H(t)$ , whereas the *dynamics* is fundamentally non-perturbative (in the sense that it cannot be described by adiabatic perturbation theory [30]). For  $U_0(t)$  there is no systematic perturbative expansion, and it is more convenient to work in a basis in which  $H_{\text{eff}}(t)$  is not diagonal, i.e.,  $\beta_n(t) = \sum_{n'=1}^M \langle z_n | U_0^\dagger(t) | z_{n'} \rangle \alpha_{n'}(t)$ . Then, Eqs. (2) and (3) yield our effective model:

$$i\dot{\beta}_n = \sum_{n'} B_{nn'} \beta_{n'}, \quad B_{nn'} = \langle z_n | H_{\text{eff}} | z_{n'} \rangle, \quad (4)$$

where in addition we dropped a sub-leading contribution  $-i \langle z_n | U_{\text{SW}} \dot{U}_{\text{SW}}^\dagger | z_{n'} \rangle$  to  $B_{nn'}$  (see [31]).

It remains to specify the explicit form of  $H_{\text{eff}}(t)$ . We separate the Hamiltonian as  $H(t) = H_0(t) + V(t)$ , where  $H_0(t)$  comprises the local longitudinal field and the four-body constraints in Eq. (1), and the perturbation  $V(t)$  is the transverse field.  $H_0(t)$  is diagonal in the states  $|z_n\rangle$ , and the perturbation  $V(t)$  flips single physical spins. In other words, applying the perturbation once to a state  $|z_n\rangle$  yields a superposition of states at a Hamming distance of one, where the Hamming distance is measured with respect to the encoded bit string  $z_n$ . The transverse field (i) modifies the energies (i.e., the diagonal elements of the effective Hamiltonian) of the states  $|z_n\rangle$  at second order in perturbation theory and (ii) couples states  $|z_n\rangle$  and  $|z_{n'}\rangle$  at the order of their Hamming distance  $h_{nn'}$ . To leading order, we find (see [31] for details)

$$\begin{aligned} H_{\text{eff},nn} &= E_0 + \langle z_n | V \frac{Q}{E_0 - H_0} V | z_n \rangle, \\ H_{\text{eff},nn'} &= \langle z_n | \left( V \frac{Q}{E_0 - H_0} \right)^{h_{nn'}-1} V | z_{n'} \rangle, \end{aligned} \quad (5)$$

where  $E_0$  is the ground state energy,  $H_0 |z_n\rangle = E_0 |z_n\rangle$ , and we introduced the projectors  $P = \sum_{n=1}^M |z_n\rangle \langle z_n|$  and  $Q = \mathbb{1} - P$ . Higher orders in the perturbative expansion of  $H_{\text{eff}}$  can be calculated through a straightforward iterative procedure [29], making it possible to approximate the full dynamics through the effective model to high precision. The constraint strengths  $C_p$  enter both  $E_0$  and  $H_0$  and thus allow us to tune the matrix elements (5).

For Hamming distances  $h_{nn'} > 2$ , the off-diagonal elements vanish faster  $\sim (1 - t/T)^{h_{nn'}}$  than the diagonal ones  $\sim (1 - t/T)^2$  as  $t \rightarrow T$ . Therefore, the instantaneous eigenstates  $|\varphi_n(t)\rangle$  converge to the states  $|x_n\rangle$  — and, in particular, not to linear combinations of these states. This corroborates that preparing a superposition of the states dynamically  $|x_n\rangle$  relies crucially on diabatic transitions.

Using the effective description, we can estimate the time  $t_d$  when the dynamics within the AMF becomes diabatic. To this end, we treat the approach of each pair of levels  $E_n(t) - E_{n'}(t) \rightarrow 0$  for  $t \rightarrow T$  as an individual Landau-Zener problem. The latter is characterized by a

time-dependent velocity and gap [32]:

$$v_{nn'} = \left| \frac{d}{dt} (H_{\text{eff},nn} - H_{\text{eff},n'n'}) \right|, \quad \Delta_{nn'} = H_{\text{eff},nn'}, \quad (6)$$

and  $t_d$  is determined by the usual criterion that separates the diabatic from the adiabatic regime in the Landau-Zener problem,  $v_{nn'}/\Delta_{nn'}^2 = \pi$ . Of all  $t_d$  found in this way for different pairs of levels  $n$  and  $n'$ , the smallest value indicates which transition becomes diabatic first. In general, transitions with higher Hamming distances have larger  $t_d$ .

Now we have all the tools at hand to determine the parameters  $C_p$  that lead to a final state  $|\psi(T)\rangle = \sum_{n=1}^M a_n |x_n\rangle$  with the required probabilities  $p_n = |a_n|^2$ . One has to calculate the ground state  $|\varphi_1(t_d)\rangle = \sum_{n=1}^M b_n |x_n\rangle$  of  $H_{\text{eff}}(t_d)$  and find the values  $C_p$  that minimize the cost function

$$\Omega(\{b_n\}) = \sum_{n=1}^M (|b_n|^2 - p_n)^2. \quad (7)$$

This gives the desired result since  $|\psi(T)\rangle \approx |\varphi_1(t_d)\rangle$  and thus  $a_n \approx b_n$  as explained above. To further improve the fidelity of the solution, one can iteratively optimize the values of the  $C_p$ . In each iteration, the time evolution with  $H_{\text{eff}}(t)$  is calculated to obtain the final state  $|\psi(T)\rangle$  beyond the sudden quench approximation, and the  $C_p$  are updated to minimize the cost function  $\Omega(\{a_n\})$  evaluated for the final state [33]. Since the optimization is carried out in the effective  $M$ -dimensional model, it can be done efficiently even if the dimension of the total Hilbert space  $2^K$  is so large that the state preparation cannot be simulated on a classical computer but still be performed on a quantum device. Thus, our protocol can provide a demonstration of computational advantages in near term quantum devices [34].

We note that the effective model, applied to the original all-to-all spin glass formulation, also provides a general framework to address the problem of fair sampling of degenerate ground states through quantum annealing [16, 18]. In particular, for spin-glass benchmark instances with controlled ground-state degeneracy, the effective model can be used to obtain the output state of quantum annealing with little computational effort. It is straightforward to extend the effective model to study the impact of, e.g., more complex driving Hamiltonians, on the composition of the output state. As we have shown here, in the lattice-gauge formulation, fair sampling can be achieved due to the additional “tuning knobs” provided by the parameters  $C_p$ .

*Example.*—Let us illustrate the method by the example shown in Fig. 1. We take  $M = 3$  bit strings  $x_1 = 1011$ ,  $x_2 = 1100$ , and  $x_3 = 1111$ . (i) These are encoded as the ground states of the Hamiltonian  $H = \sum_{i,j} J_{ij} \sigma_i^z \sigma_j^z$  with  $J_{12} = J_{13} = J_{34} = 1$ ,  $J_{23} = -1$  and  $J_{14} = J_{24} = 0$ . The

full energy landscape of  $H$  is shown in Fig. 2 (a), where the global symmetry is broken by an additional local field of strength  $h = 1$ . (ii) We switch to the lattice-gauge representation [19] featuring  $K = 6$  qubits and three constraints as depicted in Fig. 1 (c). Due to the specific arrangement of the qubits, the constraints with strengths  $C_1$  and  $C_2$  are three-body interactions and  $C_3$  is a four-body interaction (see [31] for details). Figure 2 (b) shows the time-dependent spectrum of the Hamiltonian (1) with  $C_1 = C_2 = C_3 = 4$ . (iii) For demonstration we consider two examples: we prepare superpositions of the states  $|x_n\rangle$  with target probabilities  $p_n = 1/M$  as well as  $p_1 = 0.2$ ,  $p_2 = 0.3$ , and  $p_3 = 0.5$ , see Fig. 2 (c) and (d), respectively. For equal probabilities  $p_n = 1/M$ , diagonalization of the effective Hamiltonian (see [31] for its explicit form) yields  $C_1 = 5.73$ ,  $C_2 = 0.19$ , and  $C_3 = 6.07$ . Optimizing these values iteratively we find  $C_1 = 7.91$ ,  $C_2 = 0.24$ , and  $C_3 = 8.78$ . In Fig. 2 (c), we show the exact time evolution of the squared amplitudes of the lowest three instantaneous eigenstates [35]. The optimized  $C_p$  lead to final amplitudes  $|a_1|^2 = 0.344$ ,  $|a_2|^2 = 0.347$ , and  $|a_3|^2 = 0.309$ , close to their target values. We expect further improvement by including contributions of higher order in the effective Hamiltonian. For this model, the optimization of the  $C_p$  can be carried out exactly, i.e., using the iterative procedure described above with the *full* quantum dynamics. Then we obtain  $C_1 = 9.31$ ,  $C_2 = 0.40$ , and  $C_3 = 9.82$  with final probabilities almost exactly  $1/M$  [Fig. 2 (c) solid line]. For the second example with probabilities shown in Fig. 2 (d), we obtain  $C_1 = 5.53$ ,  $C_2 = 0.86$ , and  $C_3 = 2.44$ , and by iterative optimization  $C_1 = 5.80$ ,  $C_2 = 1.25$ , and  $C_3 = 2.68$ , leading to  $|a_1|^2 = 0.219$ ,  $|a_2|^2 = 0.297$ , and  $|a_3|^2 = 0.484$ . The exact results are again almost identical to the approximate solution. In the supplemental material [31], we show that these results are also rather robust to errors in  $C_p$ . Let us stress two features of the quantum dynamics: (i) the dynamics within the AMF is evidently adiabatic, i.e., the occupation of the instantaneous ground state is constant and close to unity, up to a time  $t_d \approx 0.5$  and  $t_d \approx 0.6$  in Fig. 2 (c) and (d), respectively. (ii) This time  $t_d$  agrees well with the time at which the cost function, evaluated for the instantaneous ground state, takes its minimum — in line with the above claim that the desired state should be reached already at  $t_d$  and, in particular, prior to  $T$ .

To address how general the method is, we ask whether it is possible to reach every combination of  $|a_n|^2$  from the available parameters  $C_p$  and  $t_d$ . Let us count the number of degrees of freedom first: the number of constraints is  $K - N + 1$  which grows quadratically with the length of the bit strings  $N$ . The number of variables  $|a_n|^2$  is  $M - 1$  because of the condition  $\sum_{n=1}^M p_n = 1$ . For the example above we thus have 3 parameters and 2 degrees of freedom to program. In the supplemental

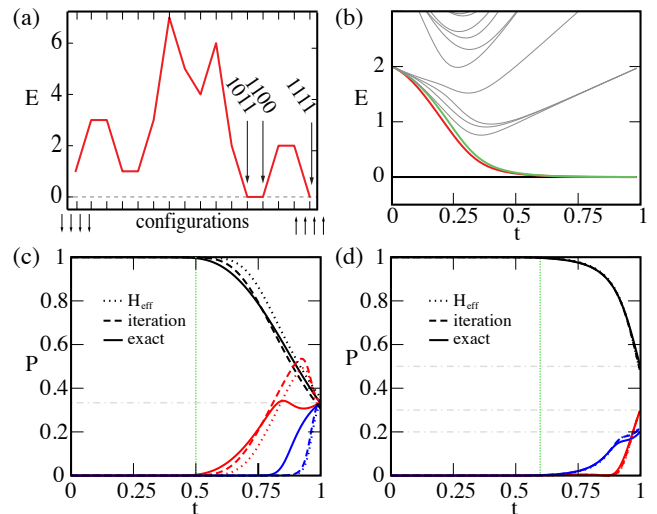


Figure 2. (a) Energy landscape of the classical spin model described in the main text, which features global minima for configurations 1011, 1100 and 1111. The symmetry of global inversion can be broken by an additional local field. (b) The energy spectrum of the time-dependent Hamiltonian Eq. (1) shows a collapse to the degenerate states (black, red and green) of the final Hamiltonian. (c) Fair sampling: probabilities of the lowest  $M$  instantaneous eigenstates of the time-dependent Hamiltonian Eq. (1) for the example shown in Fig. 1. The time of diabaticity  $t_d$  from the effective model is  $t_d \approx 0.5T$  (green dotted). The results from exact dynamics (solid), effective model (dotted) and improved iterative method (dashed) are all in good agreement. (d) Probabilities set to  $p_1 = 0.2$ ,  $p_2 = 0.3$ , and  $p_3 = 0.5$  with color code as in panel (c), where  $t_d \approx 0.6T$ .

material [31] we tested numerically for ergodicity of the solution space and see that almost all target probabilities can be reached. Since the number of parameters grows quadratically, we expect that ergodicity is even better for larger systems.

*Conclusions.*— We present a general framework that utilizes lattice-gauge degrees of freedom to control the dynamical preparation of a quantum superposition with tunable weights. The control parameters are determined from an effective multi-level Landau-Zener model. Our protocol can be implemented in state-of-the-art experiments, e.g., neutral atoms [20] or superconducting qubits [22]. From an application point of view, we hope this work is useful for quantum algorithms that benefit from data provided as superpositions [9]. The effective model also suggests a general answer to the question for the conditions of fair sampling [16, 18]. Our protocol opens several routes for extension, e.g., in combination with shortcut-to-adiabaticity methods [36–39], optimal control [40] and quantum approximate optimization algorithms [41].

*Acknowledgements.*— We thank H. Katzgraber, S. Mandra, P. Zoller, P. Hauke, H. Neven, N. Ding, M.



Mohseni, S. Gazit, M. Serbyn, and E. Altman for fruitful discussions. Research was funded by the Austrian Science Fund (FWF) through a START grant under Project No. Y1067-N27, the Hauser-Raspe foundation, and by the ERC through the synergy grant UQUAM.

---

\* [w.lechner@uibk.ac.at](mailto:w.lechner@uibk.ac.at)

- [1] J Ignacio Cirac and Peter Zoller, “Goals and opportunities in quantum simulation,” *Nat. Phys.* **8**, 264–266 (2012).
- [2] Immanuel Bloch, Jean Dalibard, and Sylvain Nascimbene, “Quantum simulations with ultracold quantum gases,” *Nat. Phys.* **8**, 267–276 (2012).
- [3] I. M. Georgescu, S. Ashhab, and Franco Nori, “Quantum simulation,” *Rev. Mod. Phys.* **86**, 153–185 (2014).
- [4] Chr. Wunderlich, Th. Hannemann, T. Körber, H. Häffner, C. F. Roos, W. Hänsel, R. Blatt, and F. Schmidt-Kaler, “Robust state preparation of a single trapped ion by adiabatic passage,” *J. Mod. Opt.* **54**, 1541–1549 (2007).
- [5] Johannes Zeiher, Rick van Bijnen, Peter Schausz, Sebastian Hild, Jae-yoon Choi, Thomas Pohl, Immanuel Bloch, and Christian Gross, “Many-body interferometry of a Rydberg-dressed spin lattice,” *Nat. Phys.* **12**, 1095–1099 (2016).
- [6] L. DiCarlo, M. D. Reed, L. Sun, B. R. Johnson, J. M. Chow, J. M. Gambetta, L. Frunzio, S. M. Girvin, M. H. Devoret, and R. J. Schoelkopf, “Preparation and measurement of three-qubit entanglement in a superconducting circuit,” *Nature* **467**, 574–578 (2010).
- [7] H. Bernien, S. Schwartz, A. Keesling, H. Levine, A. Omran, H. Pichler, S. Choi, A. S. Zibrov, M. Endres, M. Greiner, V. Vuletić, and M. D. Lukin, “Probing many-body dynamics on a 51-atom quantum simulator,” ArXiv e-prints (2017), [arXiv:1707.04344 \[quant-ph\]](https://arxiv.org/abs/1707.04344).
- [8] J. M. Raimond, M. Brune, and S. Haroche, “Manipulating quantum entanglement with atoms and photons in a cavity,” *Rev. Mod. Phys.* **73**, 565–582 (2001).
- [9] Vittorio Giovannetti, Seth Lloyd, and Lorenzo Maccone, “Quantum random access memory,” *Phys. Rev. Lett.* **100**, 160501 (2008).
- [10] Vittorio Giovannetti, Seth Lloyd, and Lorenzo Maccone, “Architectures for a quantum random access memory,” *Phys. Rev. A* **78**, 052310 (2008).
- [11] S. Lloyd, M. Mohseni, and P. Rebentrost, “Quantum algorithms for supervised and unsupervised machine learning,” ArXiv e-prints (2013), [arXiv:1307.0411 \[quant-ph\]](https://arxiv.org/abs/1307.0411).
- [12] Tadashi Kadowaki and Hidetoshi Nishimori, “Quantum annealing in the transverse ising model,” *Phys. Rev. E* **58**, 5355–5363 (1998).
- [13] E. Farhi, J. Goldstone, S. Gutmann, and M. Sipser, “Quantum Computation by Adiabatic Evolution,” ArXiv e-prints (2000), [arXiv:quant-ph/0001106 \[quant-ph\]](https://arxiv.org/abs/quant-ph/0001106).
- [14] Mohammad H. Amin, “Searching for quantum speedup in quasistatic quantum annealers,” *Phys. Rev. A* **92**, 052323 (2015).
- [15] Sergio Boixo, Vadim N. Smelyanskiy, Alireza Shabani, Sergei V. Isakov, Mark Dykman, Vasil S. Denchev, Mohammad H. Amin, Anatoly Yu Smirnov, Masoud Mohseni, and Hartmut Neven, “Computational multi-qubit tunnelling in programmable quantum annealers,” *Nat Commun* **7 SP -** (2016).
- [16] Yoshiki Matsuda, Hidetoshi Nishimori, and Helmut G Katzgraber, “Ground-state statistics from annealing algorithms: quantum versus classical approaches,” *New J. Phys.* **11**, 073021 (2009).
- [17] Sergio Boixo, Troels F. Ronnow, Sergei V. Isakov, Zhihui Wang, David Wecker, Daniel A. Lidar, John M. Martinis, and Matthias Troyer, “Evidence for quantum annealing with more than one hundred qubits,” *Nat Phys* **10**, 218–224 (2014).
- [18] Salvatore Mandrà, Zheng Zhu, and Helmut G. Katzgraber, “Exponentially biased ground-state sampling of quantum annealing machines with transverse-field driving hamiltonians,” *Phys. Rev. Lett.* **118**, 070502 (2017).
- [19] Wolfgang Lechner, Philipp Hauke, and Peter Zoller, “A quantum annealing architecture with all-to-all connectivity from local interactions,” *Science Advances* **1** (2015).
- [20] Alexander W Glaetzle, Rick MW van Bijnen, Peter Zoller, and Wolfgang Lechner, “A coherent quantum annealer with rydberg atoms,” *Nature Communications* **8** (2017).
- [21] A. Rocchetto, S. C. Benjamin, and Y. Li, “Stabilisers as a design tool for new forms of Lechner-Hauke-Zoller Annealer,” ArXiv e-prints (2016), [arXiv:1603.08554 \[quant-ph\]](https://arxiv.org/abs/1603.08554).
- [22] Shruti Puri, Samuel Boutin, and Alexandre Blais, “Engineering the quantum states of light in a kerr-nonlinear resonator by two-photon driving,” *npj Quantum Information* **3**, 18 (2017).
- [23] Martin Leib, Peter Zoller, and Wolfgang Lechner, “A transmon quantum annealer: Decomposing many-body ising constraints into pair interactions,” *Quantum Science and Technology* **1**, 015008 (2016).
- [24] Itay Hen, Joshua Job, Tameem Albash, Troels F. Ronnow, Matthias Troyer, and Daniel A. Lidar, “Probing for quantum speedup in spin-glass problems with planted solutions,” *Phys. Rev. A* **92**, 042325 (2015).
- [25] John J Hopfield, “Neural networks and physical systems with emergent collective computational abilities,” *Proceedings of the national academy of sciences* **79**, 2554–2558 (1982).
- [26] To be published.
- [27] T.W.B. Kibble, “Some implications of a cosmological phase transition,” *Phys. Rep.* **67**, 183–199 (1980); “Topology of cosmic domains and strings,” *J. Phys. A. Math. Gen.* **9**, 1387–1398 (2001); W.H. Zurek, “Cosmological experiments in superfluid helium?” *Nature* **317**, 505–508 (1985); “Cosmic Strings in Laboratory Superfluids and the Topological Remnants of Other Phase Transitions,” *Acta Phys. Pol. B* **24**, 1301 (1993); “Cosmological experiments in condensed matter systems,” *Phys. Rep.* **276**, 177–221 (1996).
- [28] Bogdan Damski, “The simplest quantum model supporting the kibble-zurek mechanism of topological defect production: Landau-zener transitions from a new perspective,” *Phys. Rev. Lett.* **95**, 035701 (2005), [arXiv:0411004 \[cond-mat\]](https://arxiv.org/abs/0411004).
- [29] Sergey Bravyi, David P. DiVincenzo, and Daniel Loss, “SchriefferWolff transformation for quantum many-body systems,” *Ann. Phys. (N. Y.)* **326**, 2793–2826 (2011).
- [30] C De Grandi and A Polkovnikov, “Quantum Quenching, Annealing and Computation,” (Springer Berlin Heidelberg, Berlin, Heidelberg, 2010) Chap. Adiabatic Pertur-

bation Theory: From Landau-Zener Problem to Quenching Through a Quantum Critical Point, pp. 75–114.

- [31] See Supplemental Material for details of the derivation of the effective model for general lattice-gauge Hamiltonians and for the example considered in the main text, as well as discussions of the robustness of the protocol to errors in the control parameters and the ergodicity of the solution space..
- [32] Landau L D and Lifshitz E M, *Quantum Mechanics: Non-relativistic Theory*, 3rd ed. (Pergamon Press, Oxford, 1977).
- [33] Note, that the minimum  $\Omega(\{a_n\}) = 0$  can only be reached if there are no transitions out of the AMF.
- [34] Sergio Boixo, Sergei V. Isakov, Vadim N. Smelyanskiy, Ryan Babbush, Nan Ding, Zhang Jiang, Michael J. Bremner, John M. Martinis, and Hartmut Neven, “Characterizing Quantum Supremacy in Near-Term Devices,” [arXiv](#) , 1–23 (2017), [arXiv:1608.00263](#).
- [35] In the lattice-gauge representation of this example, the degenerate ground states have Hamming distances  $h_{13} = h_{23} = 3$  and  $h_{12} = 4$ . Thus, as discussed below Eq. (5), the instantaneous ground states  $|\varphi_n(t)\rangle$  approach the states  $|x_n\rangle$  for  $t \rightarrow T$ , and it is indeed the probabilities of these states at  $t = T$  we want to control.
- [36] M V Berry, “Transitionless quantum driving,” *J. Phys. A Math. Theor.* **42**, 365303–9 (2009).
- [37] Sebastian Deffner, Christopher Jarzynski, and Adolfo del Campo, “Classical and Quantum Shortcuts to Adiabaticity for Scale-Invariant Driving,” *Phys. Rev. X* **4**, 021013 (2014).
- [38] Dries Sels and Anatoli Polkovnikov, “Minimizing irreversible losses in quantum systems by local counterdiabatic driving,” *Proc. Natl. Acad. Sci. U. S. A.* **114**, E3909–E3916 (2017).
- [39] Ayoti Patra and Christopher Jarzynski, “Shortcuts to adiabaticity using flow fields,” (2017), [arXiv:1707.01490](#).
- [40] T. Caneva, M. Murphy, T. Calarco, R. Fazio, S. Montangero, V. Giovannetti, and G. E. Santoro, “Optimal control at the quantum speed limit,” *Phys. Rev. Lett.* **103**, 240501 (2009).
- [41] Edward Farhi, Jeffrey Goldstone, and Sam Gutmann, “A Quantum Approximate Optimization Algorithm,” [arXiv Prepr. arXiv1411.4028](#) , 1–16 (2014), [arXiv:1411.4028](#).

# Supplemental Material: Programmable Superpositions of Ising Configurations

Lukas M. Sieberer<sup>1</sup> and Wolfgang Lechner<sup>2,3,\*</sup>

<sup>1</sup>*Department of Physics, University of California, Berkeley, California 94720, USA*

<sup>2</sup>*Institute for Theoretical Physics, University of Innsbruck, A-6020 Innsbruck, Austria*

<sup>3</sup>*Institute for Quantum Optics and Quantum Information of  
the Austrian Academy of Sciences, A-6020 Innsbruck, Austria*

(Dated: July 8, 2022)

## Abstract

We give details of the derivation of the effective model for general lattice-gauge Hamiltonians and for the example considered in the main text. We discuss the robustness of the protocol to errors in the control parameters and the ergodicity of the solution space.

## DERIVATION OF THE EFFECTIVE MODEL

Let us briefly recall the main steps in the derivation of the effective model. We decompose the total Hilbert space as  $\mathcal{H} = \mathcal{P}(t) \cup \mathcal{Q}(t)$ , where  $\mathcal{P}(t)$  is the adiabatic manifold (AMF) that is spanned by the  $M$  lowest-lying instantaneous eigenstates,  $|\varphi_n(t)\rangle$  with  $n = 1, \dots, M$ , of the lattice-gauge Hamiltonian  $H(t)$  (Eq. (1) in the main text). These states become degenerate for  $t \rightarrow T$ , and consequently the dynamics within  $\mathcal{P}(t)$  becomes diabatic, whereas a finite gap between the energies of the states in  $\mathcal{P}(t)$  and higher-lying excited states spanning the subspace  $\mathcal{Q}(t)$  is maintained throughout the protocol. Hence, transitions out of the AMF  $\mathcal{P}(t)$  can be suppressed effectively by choosing the run time  $T$  of the protocol large enough. Strictly speaking, states within  $\mathcal{P}(t)$  are also degenerate with states of  $\mathcal{Q}(t)$  at  $t = 0$ . However, the system is initialized in the instantaneous ground state which is non-degenerate at  $t = 0$  and separated from all excited states by a finite gap, so there are no diabatic transitions at short times. A state  $|\psi(t)\rangle \in \mathcal{P}(t)$  can be written in the form

$$|\psi(t)\rangle = \sum_{n=1}^M \alpha_n(t) |\varphi_n(t)\rangle, \quad (1)$$

and the Schrödinger equation, projected to  $\mathcal{P}(t)$ , reads (cf. Eq. (2) in the main text)

$$i\dot{\alpha}_n(t) = \sum_{n'=1}^M A_{nn'}(t)\alpha_{n'}(t), \quad A_{nn'}(t) = \langle \varphi_n(t) | \left( H(t) - i\frac{d}{dt} \right) | \varphi_{n'}(t) \rangle. \quad (2)$$

To make progress with the Schrödinger equation in this form we have to find the instantaneous eigenstates. As explained in the main text, the diagonalization of  $H(t)$  can be achieved in a two-step procedure: first, the space  $\mathcal{P}(t)$  of the  $M$  lowest-lying states is decoupled from excited state space  $\mathcal{Q}(t)$  by a Schrieffer-Wolff (SW) transformation  $U_{\text{SW}}(t)$ , and second the resulting effective Hamiltonian  $H_{\text{eff}}(t) = U_{\text{SW}}(t)H(t)U_{\text{SW}}^\dagger(t)$  is diagonalized within the reduced space. A detailed account of the SW transformation is given in Ref. [1], and all results for the SW we use in the following can be found there.

Apart from restricting the description of the full dynamics to the subspace  $\mathcal{P}(t)$ , a further simplification we use to derive the effective model is motivated by the observation that diabatic transitions within  $\mathcal{P}(t)$  set in only towards the end of the protocol, as can be seen for a specific example in Fig. 2 (c) and (d) in the main text. This allows us to treat the transverse field as a perturbation. In particular, we denote the unperturbed Hamiltonian



by  $H_0(t)$ . It comprises the local fields and the four-body constraints,

$$H_0(t) = \frac{t}{T} (H_J + H_C), \quad H_J = - \sum_{i=1}^K J_i \sigma_i^z, \quad H_C = - \sum_{p=1}^{K-N+1} C_p \sigma_{n_p}^z \sigma_{w_p}^z \sigma_{s_p}^z \sigma_{e_p}^z. \quad (3)$$

The perturbation is given by the transverse field  $V(t) = (1 - t/T) \sum_{i=1}^K \sigma_i^x$ , and the total Hamiltonian is

$$H(t) = H_0(t) + V(t). \quad (4)$$

At the end of the protocol, when  $t = T$ , the perturbation vanishes. We always assume that the ramp was slow enough so that the system ends up in a state within  $\mathcal{P}_0 = \mathcal{P}(T)$ , the  $M$ -dimensional ground-state manifold of  $H_0(t)$  spanned by the states  $|z_n\rangle$  with  $n = 1, \dots, M$ . Note, that  $\mathcal{P}_0$  is the ground state manifold of  $H_0(t)$  at any  $t$ , but it coincides with the AMF only at  $t = T$ . The SW transformation is a direct rotation between  $\mathcal{P}_0$  and  $\mathcal{P}(t)$ . Defining it with respect to the unperturbed Hamiltonian  $H_0(t)$ , we have  $U_{\text{SW}}(T) = \mathbb{1}$ , and at  $t < T$  the effective Hamiltonian  $H_{\text{eff}}(t) = U_{\text{SW}}(t)H(t)U_{\text{SW}}^\dagger(t)$  is block-diagonal when written in the basis of eigenstates of  $H_0(t)$ . These are simply product states in the  $\sigma^z$ -basis. Denoting the unitary transformation that diagonalizes  $H_{\text{eff}}(t)$  in  $\mathcal{P}_0$  as  $U_0(t)$ , the instantaneous eigenstates of  $H(t)$  that span  $\mathcal{P}(t)$  can be written as

$$|\varphi_n(t)\rangle = U_{\text{SW}}^\dagger(t)U_0^\dagger(t)|z_n\rangle. \quad (5)$$

Inserting this representation in Eq. (2) we find (in the following, we suppress the argument  $t$  for notational simplicity)

$$A_{nn'} = \langle z_n | \left[ U_0 \left( H_{\text{eff}} - iU_{\text{SW}}\dot{U}_{\text{SW}}^\dagger \right) U_0^\dagger - iU_0\dot{U}_0^\dagger \right] | z_{n'} \rangle, \quad (6)$$

as quoted in the main text. The SW transformation and the resulting effective Hamiltonian can be constructed explicitly as perturbative expansions. For  $U_0$  there is no such systematic procedure, and it is more convenient to work in a basis in which  $H_{\text{eff}}$  is not diagonal, i.e.,

$$\beta_n(t) = \sum_{n'=1}^M \langle z_n | U_0^\dagger(t) | z_{n'} \rangle \alpha_{n'}(t). \quad (7)$$

Then, the Schrödinger equation (2) takes the form

$$i\dot{\beta}_n(t) = \sum_{n'} B_{nn'}(t)\beta_{n'}(t), \quad B_{nn'}(t) = \langle z_n | \left( H_{\text{eff}}(t) - iU_{\text{SW}}(t)\dot{U}_{\text{SW}}^\dagger(t) \right) | z_{n'} \rangle. \quad (8)$$

When  $1/T \ll 1 - t/T \ll 1$  (note that  $T$  is the dimensionless run time of the protocol measured in units of the inverse local field strength), the second contribution to  $B_{nn'}(t)$  can be dropped: as described below, both  $H_{\text{eff}}(t)$  and  $U_{\text{SW}}(t)$  can be expressed as perturbative expansions in  $1 - t/T$ ; then, for each term of order  $(1 - t/T)^n$  in  $H_{\text{eff}}(t)$ , the corresponding term in  $U_{\text{SW}}(t)U_{\text{SW}}^\dagger(t)$  is of order  $(1/T)(1 - t/T)^{n-1} \ll (1 - t/T)^n$ . Thus, in its simplest form, the effective model is given by the equation of motion in Eq. (7) with

$$B_{nn'}(t) \approx \langle z_n | H_{\text{eff}}(t) | z_{n'} \rangle. \quad (9)$$

However, we note that including the second term in  $B_{nn'}(t)$  to make the effective model more accurate is straightforward.

## SCHRIEFFER-WOLFF TRANSFORMATION

In this section, we provide details of the perturbative calculation of the SW transformation. We follow the notation of Ref. [1].

As explained above, the SW transformation  $U_{\text{SW}}(t)$  decouples the space  $\mathcal{P}(t)$  from the space of excited states  $\mathcal{Q}(t)$  by incorporating the effect of virtual transitions to  $\mathcal{Q}(t)$  in an effective Hamiltonian  $H_{\text{eff}}(t) = U_{\text{SW}}(t)H(t)U_{\text{SW}}(t)^\dagger$ . Explicit expressions for  $H_{\text{eff}}(t)$  up to fourth order in perturbation theory are given in Ref. [1], and we repeat them here for completeness. This order of perturbation theory is sufficient for the example discussed in the main text which involves ground states with Hamming distances three and four. Higher orders — that are required to treat systems with ground states with larger Hamming distances — can be obtained through a systematic iterative procedure.

We further note, that since the qubits of the lattice-gauge representation encode the relative orientation of spins in the original all-to-all spin glass model [2], flipping a single spin of a state in  $\mathcal{P}$  always yields a state in  $\mathcal{Q}_0 = \mathcal{Q}(T)$ . For this reason, Hamming distances between ground states are at least two, and hence the lowest non-trivial order in perturbation theory that contributes to  $H_{\text{eff}}(t)$  is two. To be specific, we repeat from the main text that the transverse field (i) modifies the energies (i.e., the diagonal elements of the effective Hamiltonian) of the states  $|z_n\rangle$  at second order in perturbation theory and (ii) couples states  $|z_n\rangle$  and  $|z_{n'}\rangle$  (i.e., it generates off-diagonal elements of  $H_{\text{eff}}$ ) at order  $h_{nn'}$ , where  $h_{nn'}$  is the Hamming distance between the two states. The second effect (ii) can be understood

by noting that applying the perturbation  $V$  once to the state  $|z_n\rangle$  flips a single spin and therefore it has to be applied  $h_{nn'}$  times to connect the states  $|z_n\rangle$  and  $|z_{n'}\rangle$ .

After these preliminaries, let us specify the perturbative expansion. We denote by  $P = \sum_{n=1}^M |z_n\rangle \langle z_n|$  the projector on the ground-state manifold  $\mathcal{P}_0$ , and by  $Q = \mathbb{1} - P$  the projector on the excited state space  $\mathcal{Q}_0$ . These projectors commute with the unperturbed Hamiltonian,  $[P, H_0] = [Q, H_0] = 0$ . The ground state energy is  $E_0$ , i.e., we have  $H_0 |z_n\rangle = E_0 |z_n\rangle$ . According to Eq. (3),  $E_0$  depends linearly on time. Since the aim of the SW transformation is to decouple  $\mathcal{P}$  and  $\mathcal{Q}$ , i.e., to bring the Hamiltonian to block-diagonal form, it is useful to introduce the following superoperators:

$$\mathcal{D}(X) = PXP + QXQ, \quad \mathcal{O}(X) = PXQ + QXP. \quad (10)$$

An operator  $X$  is block-diagonal (block-off-diagonal) iff  $\mathcal{D}(X) = X$  ( $\mathcal{O}(X) = X$ ). Any operator can be decomposed into block-diagonal and block-off-diagonal components. In particular, for the perturbation we have

$$V = V_d + V_{od}, \quad V_d = \mathcal{D}(V), \quad V_{od} = \mathcal{O}(V). \quad (11)$$

Finally, for the present case in which all states in  $\mathcal{P}_0$  are degenerate, the superoperator  $\mathcal{L}$  defined in Ref. [1] takes the simple form

$$\mathcal{L}(X) = PX \frac{Q}{E_0 - H_0} - \frac{Q}{E_0 - H_0} XP. \quad (12)$$

The general form of the effective Hamiltonian to fourth order in perturbation theory is as follows:

$$\begin{aligned} H_{\text{eff}}^{(0)} &= H_0 P, \\ H_{\text{eff}}^{(1)} &= PVP, \\ H_{\text{eff}}^{(2)} &= \frac{1}{2} P[S_1, V_{od}]P, \\ H_{\text{eff}}^{(3)} &= \frac{1}{2} P[V_{od}, \mathcal{L}([V_d, S_1])]P, \\ H_{\text{eff}}^{(4)} &= \frac{1}{2} P \left( \frac{1}{4} [S_1, [S_1, [S_1, V_{od}]]] - [V_{od}, \mathcal{L}([V_d, \mathcal{L}([V_d, S_1])])]) \right) P, \end{aligned} \quad (13)$$

where  $S_1 = \mathcal{L}(V_{od})$  is the first-order term in the perturbative expansion of the generator  $S = \ln(U_{\text{SW}})$  of the Schrieffer-Wolff transformation [1].

## $H_{\text{eff}}(t)$ FOR THE EXAMPLE IN THE MAIN TEXT

In the previous section we discussed the general structure of the effective Hamiltonian and how it can be obtained systematically in a perturbative expansion. Here, we work out  $H_{\text{eff}}(t)$  explicitly for the model considered in the main text (see Fig. 1 *ibid*).

The perturbative expansion of  $H_{\text{eff}}$  is organized by the Hamming distances between the degenerate ground states — the required order of perturbation theory is determined by the maximum of the Hamming distances  $h_{nn'}$ . Also, there are some immediate simplifications: for Hamming distances three and four considered in the main text, we have  $PVP = 0$ , while  $PVQVP$  has only diagonal elements, and  $PVQVQVP$  is purely off-diagonal with non-vanishing elements between states with Hamming distance three etc. Using these simplifications we find for the example in the main text:

$$\begin{aligned}
 H_{\text{eff}}^{(0)} &= E_0 P, \\
 H_{\text{eff}}^{(1)} &= 0, \\
 H_{\text{eff}}^{(2)} &= PV \frac{Q}{E_0 - H_0} VP, \\
 H_{\text{eff}}^{(3)} &= P \left( V \frac{Q}{E_0 - H_0} \right)^2 VP, \\
 H_{\text{eff}}^{(4)} &= P \left( V \frac{Q}{E_0 - H_0} \right)^3 VP \\
 &\quad - \frac{1}{2} \left[ PV \left( \frac{Q}{E_0 - H_0} \right)^2 VPV \frac{Q}{E_0 - H_0} VP + PV \frac{Q}{E_0 - H_0} VPV \left( \frac{Q}{E_0 - H_0} \right)^2 VP \right].
 \end{aligned} \tag{14}$$

We note that  $H_{\text{eff}}^{(0)}$ ,  $H_{\text{eff}}^{(2)}$ , and the last two terms in  $H_{\text{eff}}^{(4)}$  are diagonal whereas  $H_{\text{eff}}^{(3)}$  and the first term in  $H_{\text{eff}}^{(4)}$  have non-zero elements only away from the diagonal. Numerically, we found that the diagonal contributions to  $H_{\text{eff}}^{(4)}$  have only a small effect on the dynamics, and we discard them in the following. The leading contributions take the simple form reported in the main text. If one requires increased precision, the effective Hamiltonian can be calculated systematically at higher orders through an iterative scheme [1].

While it is straightforward and most convenient to calculate  $H_{\text{eff}}(t)$  numerically, we find it instructive to obtain explicit expressions for the matrix elements of  $H_{\text{eff}}(t)$  by hand. This also clarifies how the constraint strengths  $C_p$  enter  $H_{\text{eff}}(t)$  and thus allow us to control the quantum dynamics.

For the model introduced in Fig. 1 of the main text, the part of the Hamiltonian involving the constraints involves two three-body and one four-body interaction,

$$H_C = -C_1\sigma_1^z\sigma_2^z\sigma_4^z - C_2\sigma_2^z\sigma_3^z\sigma_5^z - C_3\sigma_2^z\sigma_4^z\sigma_5^z\sigma_6^z. \quad (15)$$

Equivalently, the three-body terms can be viewed as four-body terms in which one spin is held fixed, e.g., by an external field [2]. We denote by  $S_i$  the set of constraints that involve spin  $i$ ,

$$S_1 = \{1\}, \quad S_2 = \{1, 2, 3\}, \quad S_3 = \{2\}, \quad S_4 = \{1, 3\}, \quad S_5 = \{2, 3\}, \quad S_6 = \{3\}. \quad (16)$$

The energy of the degenerate ground states  $|z_n\rangle$  is

$$E_0 = -\frac{t}{T} \left( \sum_i J_i z_{n,i} + \sum_{p=1}^3 C_p \right), \quad (17)$$

where the contribution due to the local fields depends on the orientation of the spins  $z_{n,i}$  (here, we replace  $z_{n,i} = 0, 1 \rightarrow \pm 1$ ), while each constraint contributes with  $-tC_p/T$  for states in the ground-state manifold.

We obtain the diagonal elements of  $H_{\text{eff}}$  at second-order in perturbation theory:

$$\begin{aligned} H_{\text{eff},nn} &= E_0 + \left(1 - \frac{t}{T}\right)^2 \sum_{i,j} \langle z_n | \sigma_i^x \frac{1}{E_0 - H_0} \sigma_j^x | z_n \rangle \\ &= E_0 + \left(1 - \frac{t}{T}\right)^2 \sum_i \frac{1}{E_0 - \langle z_n | \sigma_i^x H_0 \sigma_i^x | z_n \rangle}. \end{aligned} \quad (18)$$

Here we used that the state  $\sigma_i^x |z_n\rangle$  is still a product state in the  $\sigma^z$ -basis (only with spin  $i$  flipped relative to  $|z_n\rangle$ ), and  $H_0$  is diagonal in this basis. The excitation energy of the state  $\sigma_i^x |z_n\rangle$  is given by

$$\langle z_n | \sigma_i^x H_0 \sigma_i^x | z_n \rangle - E_0 = \frac{2t}{T} \left( J_i z_{n,i} + \sum_{p \in S_i} C_p \right), \quad (19)$$

i.e., we get a contribution from the local field acting on spin  $i$  and from all the constraints that involve this same spin. These constraints are satisfied in the state  $|z_n\rangle$  and therefore violated if the single spin  $i$  is flipped. Hence,

$$H_{\text{eff},nn} = E_0 - \frac{T}{2t} \left(1 - \frac{t}{T}\right)^2 \sum_i \frac{1}{J_i z_{n,i} + \sum_{p \in S_i} C_p}. \quad (20)$$



For the off-diagonal elements  $H_{\text{eff},nn'}$  there is no equally compact form. However, they can be visualized in an intuitive way as shown in Fig. 1. The key observation is that a given order of the perturbation, applied to a state  $|z_{n'}\rangle$  leads to “paths” originating from this state. The length of these paths is the number of single spin flips to go from one state to the other. The order of the perturbations is determined by this length: to leading order, those paths contribute to  $H_{\text{eff},nn'}$  that connect the states  $|z_{n'}\rangle$  and  $|z_n\rangle$  in the minimum number of steps. This number is given by the Hamming distance  $h_{nn'}$  of these states. We formalize these considerations in the following.

Let’s denote the spins we have to flip to get from  $|z_{n'}\rangle$  to  $|z_n\rangle$  by  $D = (i_1, i_2, \dots, i_h)$  with  $h = h_{nn'}$ . The paths that contribute to  $H_{\text{eff},nn'}$  are different sequences of spin flips, i.e., permutations of  $D$ . We denote such a permutation by  $\pi(D) = (i_{\pi_1}, \dots, i_{\pi_h})$ . There are  $h!$  permutations. For a given permutation, the repeated action of the perturbation  $V$  takes us through the sequence of states

$$|z_{n'}\rangle \rightarrow \sigma_{i_{\pi_1}}^x |z_{n'}\rangle \rightarrow \sigma_{i_{\pi_2}}^x \sigma_{i_{\pi_1}}^x |z_{n'}\rangle \rightarrow \dots \rightarrow \sigma_{i_{\pi_h}}^x \dots \sigma_{i_{\pi_1}}^x |z_{n'}\rangle = |z_n\rangle. \quad (21)$$

Using the same notation as in Eq. (18), we find

$$H_{\text{eff},nn'} = (-1)^h \left(1 - \frac{t}{T}\right)^h \sum_{\pi} \frac{1}{E_0 - \langle z_{n'} | \sigma_{i_{\pi_1}}^x \dots \sigma_{i_{\pi_{h-1}}}^x H_0 \sigma_{i_{\pi_h}}^x \dots \sigma_{i_{\pi_1}}^x | z_{n'} \rangle} \times \dots \frac{1}{E_0 - \langle z_{n'} | \sigma_{i_{\pi_1}}^x H_0 \sigma_{i_{\pi_1}}^x | z_{n'} \rangle}. \quad (22)$$

The constraint strengths  $C_p$  enter this expression through the energy denominators as above in Eq. (20). While Eqs. (20) and (22) provide valuable insight into the general structure of the effective model, for doing any practical calculation it is much simpler to directly implement Eq. (14), e.g., in MATHEMATICA. Doing this for our model, we find that the effective Hamiltonian can be written as

$$H_{\text{eff},nn} = E_0 + \frac{T}{t} \left(1 - \frac{t}{T}\right)^2 e_n, \quad H_{\text{eff},nn'} = \left(\frac{T}{t}\right)^{h_{nn'}-1} \left(1 - \frac{t}{T}\right)^{h_{nn'}} g_{nn'}, \quad (23)$$

with the following coefficients on the diagonal:

$$\begin{aligned} e_1 &= \frac{1}{2} \left( -\frac{1}{1+C_2} - \frac{1}{C_3} - \frac{1}{1+C_1+C_3} - \frac{1}{C_2+C_3} + \frac{1}{1-C_1-C_2-C_3} - \frac{1}{1+C_1} \right), \\ e_2 &= \frac{1}{2} \left( -\frac{1}{1+C_2} - \frac{1}{C_3} + \frac{1}{1-C_1-C_3} - \frac{1}{C_2+C_3} - \frac{1}{1+C_1+C_2+C_3} - \frac{1}{1+C_1} \right), \\ e_3 &= \frac{1}{2} \left( -\frac{1}{1+C_2} - \frac{1}{C_3} - \frac{1}{1+C_1+C_3} - \frac{1}{C_2+C_3} - \frac{1}{1+C_1+C_2+C_3} + \frac{1}{1-C_1} \right), \end{aligned} \quad (24)$$

and on the off-diagonal:

$$\begin{aligned}
g_{13} &= \frac{1}{2^2} \left( -\frac{\frac{1}{C_2+C_3} + \frac{1}{1+C_1}}{1+C_1+C_2+C_3} - \frac{\frac{1}{1-C_1-C_2-C_3} - \frac{1}{C_2+C_3}}{1-C_1} + \frac{\frac{1}{1-C_1-C_2-C_3} - \frac{1}{1+C_1}}{C_2+C_3} \right), \\
g_{23} &= \frac{1}{2^2} \left( -\frac{\frac{1}{1+C_1} + \frac{1}{C_3}}{1+C_1+C_3} + \frac{\frac{1}{1-C_1-C_3} - \frac{1}{1+C_1}}{C_3} - \frac{\frac{1}{1-C_1-C_3} - \frac{1}{C_3}}{1-C_1} \right),
\end{aligned} \tag{25}$$

and

$$\begin{aligned}
g_{12} &= \frac{1}{2^3} \left( \frac{-\frac{\frac{1}{C_2+C_3} + \frac{1}{1+C_1+C_3}}{1+C_1+C_2} + \frac{\frac{1}{1-C_1-C_2-C_3} - \frac{1}{1+C_1+C_3}}{C_2} - \frac{\frac{1}{1-C_1-C_2-C_3} - \frac{1}{C_2+C_3}}{1-C_1}}{C_3} \right. \\
&\quad - \frac{-\frac{\frac{1}{C_2+C_3} - \frac{1}{C_3}}{C_2} - \frac{\frac{1}{1-C_1-C_2-C_3} - \frac{1}{C_2+C_3}}{1-C_1} - \frac{\frac{1}{1-C_1-C_2-C_3} - \frac{1}{C_3}}{1-C_1-C_2}}{1-C_1-C_3} \\
&\quad + \frac{-\frac{\frac{1}{1+C_1+C_3} + \frac{1}{C_3}}{1+C_1} + \frac{\frac{1}{1-C_1-C_2-C_3} - \frac{1}{1+C_1+C_3}}{C_2} - \frac{\frac{1}{1-C_1-C_2-C_3} - \frac{1}{C_3}}{1-C_1-C_2}}{C_2+C_3} \\
&\quad \left. + \frac{-\frac{\frac{1}{1+C_1+C_3} + \frac{1}{C_3}}{1+C_1} - \frac{\frac{1}{C_2+C_3} + \frac{1}{C_3}}{C_2} - \frac{\frac{1}{C_2+C_3} + \frac{1}{1+C_1+C_3}}{1+C_1+C_2}}{1+C_1+C_2+C_3} \right). \tag{26}
\end{aligned}$$

The representation of these coefficients as iterated fractions directly reflects the structure of perturbation theory, see Fig. 1.

Finally, we note that while formally we treat  $1 - t/T$  as the expansion parameter, we found that we obtain a more accurate description of the system dynamics if we keep the factors  $t/T$  that appear in the energy denominators in the above expansion of  $H_{\text{eff}}$  and do not replace them by  $t/T \approx 1$  which would strictly speaking be necessary to obtain a consistent expansion. Due to these factors, the perturbative expansion diverges for  $t \rightarrow 0$ . This, however, turns out to not be a severe obstacle in practice: for the iterative optimization of the constraint strengths  $C_p$  described in the main text, we initialize the time evolution at a finite time  $t_0 > 0$  in the instantaneous ground state  $|\varphi_1(t_0)\rangle$ . In the examples we considered, we found that the optimized  $C_p$  are almost insensitive to the value of  $t_0$  for  $0 < t_0 \lesssim t_d$ .

## ROBUSTNESS TO CONSTRAINT ERRORS

The framework described in the main text allows one to program the probabilities  $p_n = |a_n|^2$  of a superposition  $|\psi\rangle = \sum_{n=1}^M a_n |x_n\rangle$  by tuning the constraint strengths  $C_p$ . The physical protocol that allows one to create the superposition is based on an adiabatic passage with controlled diabatic transitions within the adiabatic manifold. Here we address

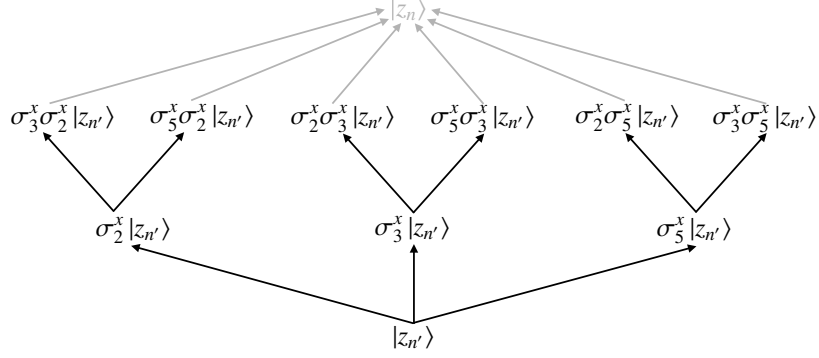


Figure 1. Graphical representation of an off-diagonal element of the effective Hamiltonian. We consider an example in which two of the degenerate ground states of  $H_0$  are given by  $|z_n\rangle = |010011\rangle$  and  $|z_{n'}\rangle = |001001\rangle$ , i.e., they have Hamming distance  $h_{nn'} = 3$ . In particular,  $|z_n\rangle$  can be obtained from  $|z_{n'}\rangle$  by flipping the spins at positions 2, 3, and 5,  $|z_n\rangle = \sigma_2^x \sigma_3^x \sigma_5^x |z_{n'}\rangle$ . Then, there is an off-diagonal matrix element  $H_{\text{eff},nn'}$  in third order in perturbation theory. The terms contributing to this matrix element can be visualized as sums over paths connecting the states  $|z_n\rangle$  and  $|z_{n'}\rangle$ . Each path corresponds to a particular order in which the spins 2, 3, and 5 are flipped, and each segment of a given path contributes with a factor of minus one over the excitation energy of the state at the end of the segment. The tree-like structure in the figure translates directly to the iterated fractions, e.g., in the expression for  $g_{13}$  in Eq. (25). Indeed, comparing the first term in  $g_{13}$  and the left-most branch of the tree, we see that flipping spin 2 leads to a state with excitation energy  $2(1 + C_1 + C_2 + C_3)$ ; depending on which spin is flipped next, states with energies of  $2(1 + C_1)$  or  $2(C_2 + C_3)$  are reached. The last segment of the path that leads to  $|z_n\rangle$  does not contribute to the matrix element  $H_{\text{eff},nn'}$  as is indicated in the figure by reduced opacity.

the question how sensitive the final probabilities are with respect to errors in the control parameters  $C_p$ . We define the relative error  $e$ , where  $\hat{C}_p = eC_p$ , and  $C_p$  are the constraints obtained by optimization as explained in the main text. For the example given in Fig. 1 *ibid* and target probabilities  $p_n = 1/M$ , the values for  $C_p$  are taken from the exact calculation in the main text. The changes in the probabilities for  $e$  ranging from 0.6 to 1.4 are shown in Fig. 2. Around  $e = 1$ , the solution is remarkably insensitive to errors.

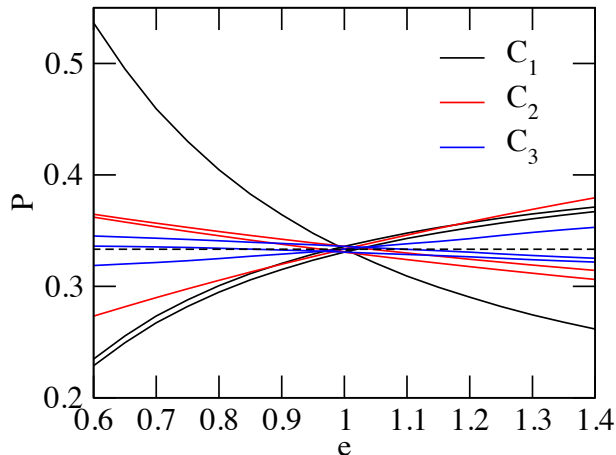


Figure 2. Probabilities  $P$  of the final superposition as a function of the relative error in the constraints  $e$ . We consider the example shown in Fig. 1 in the main text with equal target probabilities including errors in  $C_1$  (black),  $C_2$  (red) and  $C_3$  (blue). The three lines of each color show the probabilities  $|a_1|^2$ ,  $|a_2|^2$ , and  $|a_3|^2$ , respectively. For the constraint most sensitive to errors, i.e.  $C_1$ , the error in  $P$  is 10 % for a error of 20 % in  $C_1$ . For other constraints the error in  $P$  is even smaller.

## ERGODICITY OF THE SOLUTION SPACE

In this section we address the question whether we can program all possible superpositions by variation of the constraints. To this end, we regard the protocol described in the main text as a mapping from constraint strengths  $C_p$  to superposition probabilities  $p_n$ . Let us first compare the number of degrees of freedom that we want to program to the number of parameters. The number of parameters is  $K$ , the number of constraints, and grows quadratically with the length of the bit strings [2]. On the other hand, the number of degrees of freedom that we want to program is the number of bit strings  $M$ . As the state must be normalized, there is a condition that  $\sum_{n=1}^M p_n = 1$ . Therefore,  $M - 1$  degrees of freedom need to be programmed and  $K$  degrees of freedom are available. This means, that for large systems the number of available parameters will in general be large as compared to number of variables that we want to program. For small systems we can systematically address the question whether the solution hyperplane is ergodically populated from all constraint combinations. In the example considered in the main text, the number of bit strings is  $M = 3$ . With the condition  $p_1 + p_2 + p_3 = 1$ , the solution space is a 2D plane in the

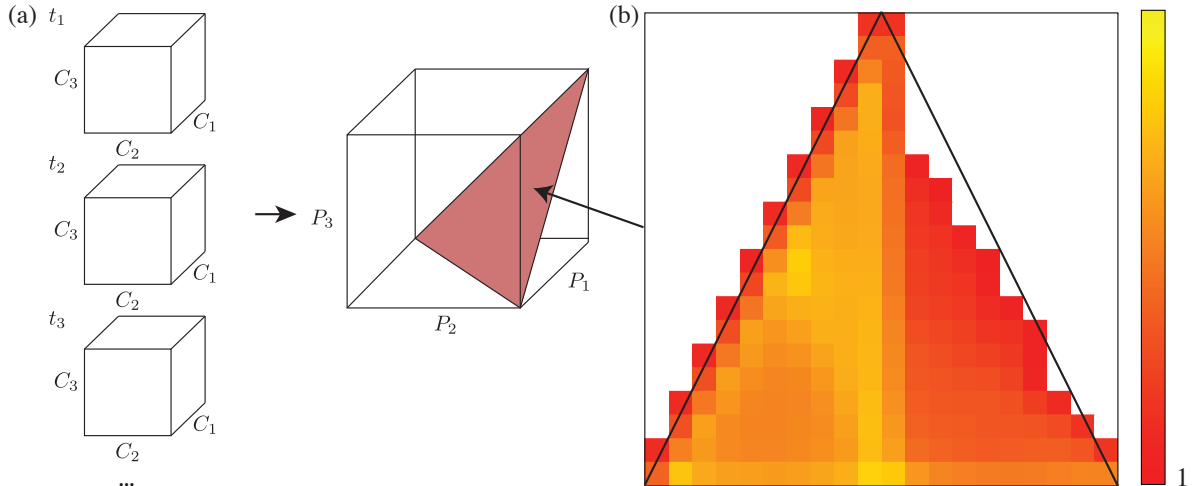


Figure 3. (a) The protocol described in the main text maps the parameter set  $\{t_d, C_1, C_2, C_3\}$  to a 2D plane in the solution space spanned by  $\{p_1, p_2, p_3\}$ . The mapping is ergodic, if each point on this plane can be reached. (b) Heatmap of the projected probabilities on the 2D solution plane. Points that can be reached (red) are all within the expected triangle, while a small region in the top right (white) cannot be reached.

three-dimensional space of probabilities. We can systematically check how this 2D plane is populated from the following simplified model, illustrated in Fig. 3 (a). According to the effective model in the main text, we assume that the amplitudes in the instantaneous ground state stay constant after the a certain freezing time. We assume that the freeze-in can be at any time during the protocol. Therefore, we can check each combination of  $C_1$ ,  $C_2$  and  $C_3$  for each time  $t_d$ . We scan the constraints in the interval 0.1 to 4.0 in steps of 0.1 and the time in steps of  $T/30$ . The resulting solution plane is shown in Fig. 3 (b). The mapping is almost ergodic even in this simplified model. For larger systems we expect full ergodicity due to the larger number of degrees of freedom.

---

\* [w.lechner@uibk.ac.at](mailto:w.lechner@uibk.ac.at)

[1] Sergey Bravyi, David P. DiVincenzo, and Daniel Loss, “SchriefferWolff transformation for quantum many-body systems,” *Ann. Phys. (N. Y.)*. **326**, 2793–2826 (2011).



- [2] Wolfgang Lechner, Philipp Hauke, and Peter Zoller, “A quantum annealing architecture with all-to-all connectivity from local interactions,” [Science Advances](#) **1** (2015).